

# Pinion development of face-milled spiral bevel and hypoid gears based on contact attributes

Yu Yang<sup>1</sup> · Shimin Mao<sup>1</sup> · Wenchao Guo<sup>1</sup> · Yuhua Kuang<sup>1</sup>

Received: 19 June 2015 / Accepted: 21 September 2015 / Published online: 1 October 2015  
© Springer-Verlag London 2015

**Abstract** This paper proposes a pinion development approach in order to obtain excellent transmission performance of the face-milled spiral bevel and hypoid gears. First, the flank form of the gear pair is determined based on the original designed ease-off topography by adjusting the contact attributes. After the gear pair is finished and measured, the deviation sum can be established by converting the wheel flank deviations into the equivalent pinion flank deviations. Then, the real ease-off topography is obtained, which is an important indicator to evaluate the transmission performance. Next, the real ease-off topography is redesigned with the target of the original designed ease-off topography to compensate the deviation sum by readjusting the contact attributes. Thus, the pinion flank form is redesigned and the corresponding machine-tool settings can be calculated by the active design method. According to which, the pinion is recut/reground and the wheel remains unchanged. Finally, the approach is conducted on a face-milled hypoid gear pair to demonstrate its effectiveness.

**Keywords** Spiral bevel and hypoid gear · Contact attributes · Ease-off · Active design · Face-milled

## 1 Introduction

Face-milled spiral bevel and hypoid gears are essential transmission components in vehicles. When the macroscopic geometric parameters of a bevel gear pair are determined, like number of teeth, module, pressure angle, and spiral angle, the microscopic geometry of the tooth flank determines the transmission performance of this gear pair and then influences the performance of the product, such as lifetime, noise, vibration, load capacity, and so on.

In practice, with the transmission system under load and the temperature variation during operation, the deformation of gear teeth, shafts, some other parts in box, and box itself will occur. At the same time, the misalignments of gear pair exist because of assembling deviation and component deviation. As a result, load concentration will arise if the mated tooth surfaces are in complete conjugation, which is detrimental to all performance parameters of this gear pair [1]. Therefore, the mismatched tooth flank is always used instead of fully conjugated tooth flank for better performance [2–5].

The contact behavior of a gear pair is determined by the microscopic geometry (modification form) of the tooth flank, which is determined by ease-off topography. In other words, ease-off topography is an indicator of measuring flank modification. Different ease-off topography figures correspond to different flank modification forms, and different transmission performances follow.

Due to some inevitable reasons, however, such as, machine axis motion error, tool error, fixture error, thermal deformation, and so on, there are always flank deviations. Consequently, the real ease-off topography deviates from the designed one, so flank deviations need to be taken into account in the stage of ease-off design.

Some works related to this problem have been conducted. The minimization of the entire tooth surface deviations by the

---

✉ Shimin Mao  
maosm@mail.xjtu.edu.cn

<sup>1</sup> School of Mechanical Engineering, State Key Laboratory for Manufacturing Systems Engineering, Xi'an Jiaotong University, Xi'an, Shaanxi 710049, People's Republic of China

least-square method was given by Litvin et al. [6]. With the linear regression method and the sensitivity matrix applied, Lin et al. [7] corrected the machine-tool settings to minimize the flank deviations, and later, they improved the optimization using the SQP method in [8]. The high-order flank-correction method was developed by Shih et al. [9, 10] based on the five-axis CNC gear profile grinding machine and the six-axis CNC hypoid generator. Fan [11, 12] determined the corrective universal motion coefficients utilizing the universal motions for face-milled and face-hobbed spiral bevel and hypoid gears. A new systematic method for modifying gear tooth flank with proper variations in the machine-tool settings was presented by Artoni et al. [13], with the problem solved by the Levenberg–Marquardt method. Yang et al. [14] also corrected the pinion tooth surface deviations only for spiral bevel and hypoid gears by SGM method.

The tooth contact analysis of spiral bevel gears was developed by Gleason Works [15]. Shih and Fong [16, 17] proposed the flank modification methodology using a linear regression method, based on the desired ease-off topographies and the sensitivity matrix. Artoni et al. [18] proposed a fully automatic procedure to optimize the loaded tooth contact pattern by two steps: identification of the coefficients of the optimal ease-off surface and that of the machine setting corrections required to generate it. A new load distribution model was proposed to simulate contact conditions of both face-milled and face-hobbed hypoid gears produced by Formate and generate processes by Kolivand et al. [19]. A practical methodology based on ease-off topography is proposed by Kolivand et al. [20] for loaded tooth contact analysis of hypoid gears having both local and global deviations. A new hypoid gear mechanical efficiency model was proposed by Kolivand et al. [21], and the influence of various design and operating parameters on mechanical efficiency of a hypoid gear pair was quantified. The influence of tooth modifications induced by machine-tool setting and head-cutter profile variations on tooth contact characteristics in face-hobbed spiral bevel gears is investigated by Simon [22]. A microgeometry optimization method of face-hobbed hypoid gear set aiming at enhancing gear performance was presented by Artoni et al. [23] with a general algorithmic framework for ease-off multi-objective optimization. Artoni et al. [24] applied corrective actions to the pinion member only by mapping gear deviations into equivalent pinion deviations. Simon defined optimal tooth modifications of face-hobbed spiral bevel gears by appropriately chosen head-cutter geometry and machine-tool setting to reduce the maximum tooth contact pressure and transmission errors in face-hobbed spiral bevel gears in [25].

This paper aims to propose a pinion development approach based on contact attributes. First, the predesigned theoretical ease-off topography is determined. Then, with the flank deviations of the gear pair considered, the redesigned real ease-off topography is obtained. By this, the pinion is redesigned.

Finally, the corresponding machine-tool settings are determined by the active design method. This paper deals with hypoid gears by half generating method, that is, the wheel flank is produced by the Formate method and the pinion flank is generated by rolling. The modification to provide localized contact pattern of this enveloped surface is the goal of this research.

## 2 Logic flow of development

In this section, the logic flow of the development is described. As Fig. 1 shows, it contains two parts: original design stage and pinion redesign stage.

In the original design stage, the wheel flank form is designed first and the wheel design remains unchanged. In order to obtain excellent performance, three contact attributes are

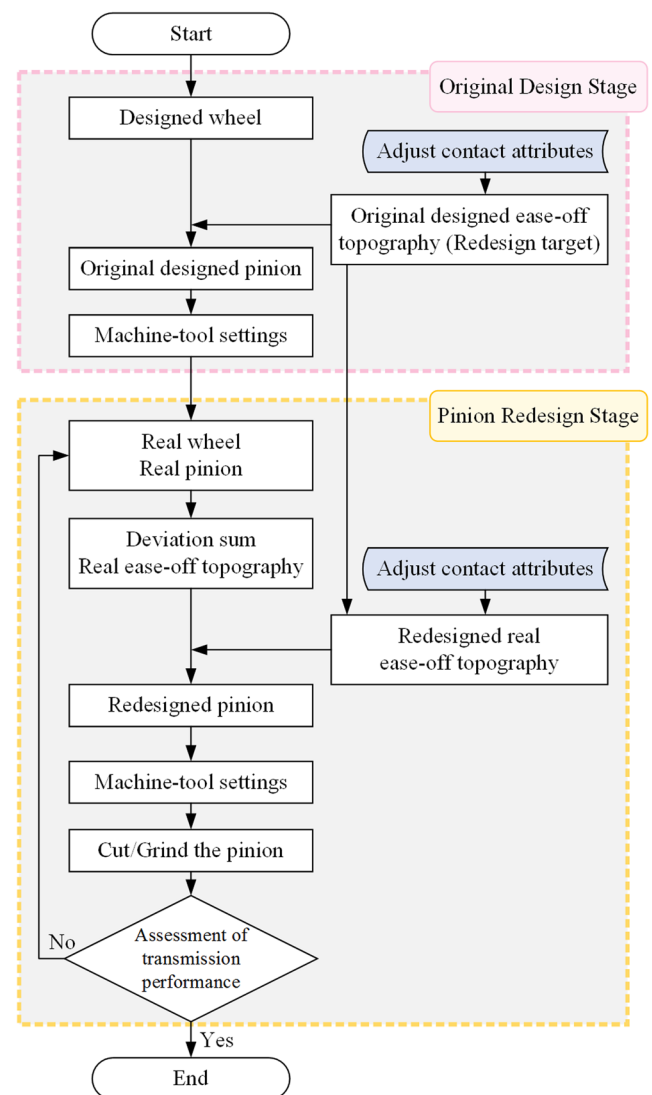


Fig. 1 The Logic flow of development

adjusted, and then the original designed ease-off topography is established, which is the target in the second part. Thus, the original design of the pinion flank form is determined.

In the pinion redesign stage, the gear pair is cut/ground on the machine according to the original design and subsequently measured on the coordinate measuring machine (CMM). Then, with the flank deviations obtained, the deviation sum and the real ease-off topography are derived. To improve the transmission performance, the contact attributes are readjusted with the goal that the redesigned real ease-off topography is close to the original designed ease-off topography. In this way, the flank form of the pinion redesigned. Finally, the machine-tool settings are recalculated and the pinion is cut/ground again. This stage is conducted until the transmission performance meets requirement.

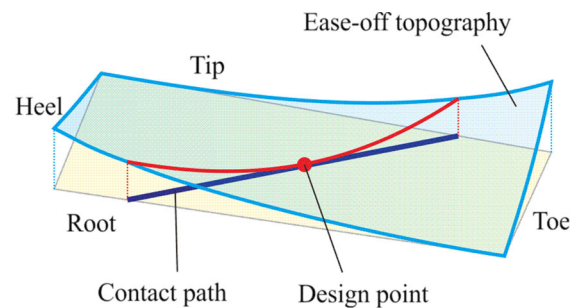
### 3 Original design stage

#### 3.1 Definition of ease-off

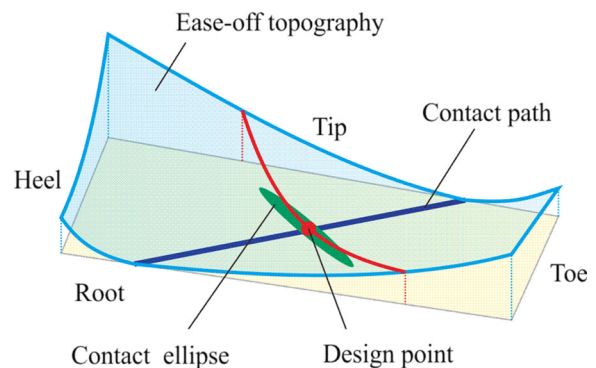
When the wheel flank is given, there is a unique fully conjugated pinion flank which meshes with the wheel flank in line contact by the theoretical constant transmission ratio  $z_w/z_p$ , where  $z_w$  is the number of the wheel teeth and  $z_p$  is the number of the pinion teeth, whereas, in order to obtain local contact between the gear pair, the pinion flank is modified according to certain design rules. Hence, the modified pinion flank deviates from the fully conjugated one, and ease-off is used to describe the deviations between these two flanks.

The tooth flank is divided into a grid and defined by a series of discrete points. Ease-off value denotes the deviation value in normal direction at each grid point. If the value is positive, the modified flank has less material relative to the fully conjugated one at this grid point; if negative, more material. And for local contact, it can be regarded that the modified flank is the fully conjugated flank with the ease-off quantity material removed from, so the designed ease-off value is always positive. Ease-off topography represents the set of ease-off values at all grid points, describing the modification of the overall flank of the pinion member. As Fig. 2 shows, the plane below (yellow) stands for the fully conjugated pinion flank and the upper curved surface (blue) stands for the ease-off topography.

If the pinion is not modified, the ease-off topography will coincide with the plane below and the ease-off value at each grid point will be zero. At the same time, the fully conjugated flanks mesh with each other with zero transmission error (TE), and there is an infinite long instantaneous contact line at each rolling angle. During the period from starting meshing to ending meshing of one pair of mated flanks, the contact line moves along the contact path.



(a) Modification along contact path only



(b) Modification along contact line only

**Fig. 2** Ease-off topography based on contact attributes. **a** Modification along contact path only; **b** modification along contact line only

#### 3.2 Original design of the pinion

To design the flank form of the pinion, three contact attributes can be controlled, that is, the position and direction of the contact path, the transmission error, and the major axis of the instantaneous contact ellipse at the design point.

First, it is necessary to design the position and direction of the contact path, on which a “design point” is determined simultaneously, usually in the vicinity of the midpoint of the contact path. This step makes a difference to the position and shape of the contact pattern. Where the contact path locates, there is less material pared off relative to other area on pinion flank and the ease-off value here is less too. As the contact path get close to the face width direction, the contact path get longer and the contact ratio get greater.

The next step is to adjust the transmission error. As mentioned above, the transmission error is zero before modification, and it is designed to be a parabolic function along the contact path here, with the highest point of the parabola and the “design point” coinciding. In this case, there exists only one point with zero transmission error, which is the “design point”. Then the gear pair will match with each other based on the designed changeable transmission ratio instead of the constant one. For reaching this effect, the pinion flank is modified along the contact path and then the ease-off value along the

contact path can be determined, as Fig. 2a shows. The greater the maximal transmission error, the greater the ease-off value along the contact path.

After the last step, though the pinion flank is modified along the contact path, the mated flanks are still in line contact, just with a changeable transmission ratio, and the major axis of the instantaneous contact ellipse is infinitely great. In order to obtain a local contact pattern, the pinion flank also needs to be modified along the instantaneous contact line, and to achieve that, the major axis of the contact ellipse is shortened to a limited length. In fact, only the major axis at the “design point” is controlled, and the major axis at other points will be shortened to the approximate length accordingly. Consequently, the mated flanks are changed into point contact from line contact. At every rolling angle, the wheel flank and the pinion flank contact at one corresponding point on the contact path. With continuous rotation, all the instantaneous contact points constitute the contact path. The boundary of the contact ellipse is determined on the condition that the normal distance between the mated flanks equals  $6.35\ \mu\text{m}$ . The shorter the major axis, the narrower the contact pattern and the greater the ease-off value along the contact line. Figure 2b illustrates the situation that the modification is only along the contact line, with zero modification on the contact path.

The demands of the contact attributes influence the form of the ease-off topography, and in return, the ease-off topography plays an important role on the contact performance of gear pair. Consequently, with the ease-off topography designed, the original design of the pinion flank form is determined.

### 3.3 Determination of machine-tool settings

According to the thought of function-oriented active tooth surface design [26], the form of the tooth surface is free of the limitation of the traditional cradle style machine and the tooth surface with excellent meshing behaviors can be easily obtained. Therefore, after the pinion flank form is determined, the corresponding machine-tool settings can be obtained by solving an equation set according to the active design method. That is, the cutter radius for cutting/grinding the pinion and a series of motion coefficients of each axis of the 5-axis CNC machine can be determined. Then, the gear pair can be cut/grind.

## 4 Pinion redesign stage

### 4.1 Deviation sum of the real gear pair

After finished, the gear pair can be measured on CMM and the flank deviations are obtained. Since the contact performance is affected by both the wheel and the pinion flank deviations, both the wheel flank deviations and the pinion flank

deviations need to be taken into consideration in the pinion redesign stage.

In addition, the bevel gears are manufactured and used in pair in most cases, so the wheel flank deviations can be converted into the equivalent pinion flank deviations. Thus, the wheel flank deviations and the pinion flank deviations can be expressed together, in the form of deviation sum. And it can be obtained as follows.

$$\delta^{(S)}(i, j) = \delta^{(W)}(i, j) + \delta^{(P)}(i, j) \quad (1)$$

where  $\delta^{(W)}(i, j)$  denotes the normal deviation at the grid point in the  $i^{\text{th}}$  row and the  $j^{\text{th}}$  column on the wheel flank, and  $\delta^{(P)}(i, j)$  denotes the normal deviation at the grid point in the  $i^{\text{th}}$  row and the  $j^{\text{th}}$  column on the pinion flank. It is worth noting that the point  $(i, j)$  on the wheel flank and the point  $(i, j)$  on the pinion flank are nearly meshing points. This is accomplished by three steps: (1) calculating the position vector of the pinion point which meshes with the grid point  $(i, j)$  on the wheel flank in complete conjugation by the constant transmission ratio; (2) determining the grid coordinate of the pinion point obtained in step (1) in the rotation projection coordinate system; (3) calculating the position vector of the point  $(i, j)$  on the designed pinion flank according to the grid coordinate determined in step (2).

For all the deviations, positive value means redundant material relative to the nominal flank at that grid point, and negative means less. Before doing this, the singular feature points at which the deviation is not normal should be smoothed.

### 4.2 Real ease-off topography

As mentioned above, when those three contact attributes above are designed, the ease-off topography can be established and then the microscopic geometry (modification form) of the pinion tooth flank is determined. In other words, the ease-off topography determines the contact performance of the gear pair. If the flank deviations and assembly errors are not taken into account, the gear pair will mesh according to the predesigned contact demands. Nonetheless, flank deviations are inevitable, thus the ease-off topography between the real pinion flank and the fully conjugated pinion flank, which matches with the real wheel flank, is not as the same as the predesigned one, and it is called “real ease-off topography” here. Therefore, the contact performance will get detrimentally affected.

The real ease-off value at each point can be calculated as follows:

$$\xi^{(\text{Real})}(i, j) = \xi^{(O)}(i, j) - \delta^{(S)}(i, j) \quad (2)$$

where  $\xi^{(O)}(i, j)$  is the original predesigned ease-off value at point  $(i, j)$  and  $\delta^{(S)}(i, j)$  is the deviation sum at point  $(i, j)$ .

### 4.3 Redesign target

With the deviation sum taken into account during the ease-off topography design, the real ease-off topography can be designed directly. Therefore, the deviation sum can be compensated on the pinion member only for cost and time saving.

The desired redesigned ease-off value at each grid point  $(i, j)$  can be achieved by the following equation:

$$\xi^{(\text{Redesign})}(i, j) = \xi^{(O)}(i, j) + \delta^{(S)}(i, j) \tag{3}$$

The ease-off topography composed by all the  $\xi^{(\text{Redesign})}$  values is called  $\Sigma^{(\text{Redesign})}$ , and the corresponding flank is called “desired redesigned flank”.

The desired redesigned real ease-off value at each grid point  $(i, j)$  of the desired redesigned flank can be derived as follows:

$$\begin{aligned} \xi^{(\text{Redesign Real})}(i, j) &= \xi^{(\text{Redesign})}(i, j) + \delta^{(S)}(i, j) \\ &= \xi^{(O)}(i, j) + \delta^{(S)}(i, j) - \delta^{(S)}(i, j) \\ &= \xi^{(O)}(i, j) \end{aligned} \tag{4}$$

The ease-off topography composed by all the  $\xi^{(\text{Redesign Real})}$  values is called  $\Sigma^{(\text{Redesign Real})}$ , and it is the desired real ease-off topography of the desired redesigned flank, which is the redesign target. This is under the assumed condition that the work piece is cut/ground on the same machine in a steady state so that the flank deviations are stable.

### 4.4 Pinion redesign

With the “desired redesigned real ease-off topography” as the target, the pinion flank form can be redesigned. Those three contact attributes are adjusted to make sure that the simulated real ease-off topography get very close to the target  $\Sigma^{(\text{Resign Real})}$ . *The final adjustment result can be determined by comparing the ease-off values as well as the position of the lowest part. After the redesign of the pinion, there might be little difference between each redesigned ease-off value and each corresponding target value, but their overall trends accord.*

After the determination of the redesigned three contact attributes, the first-order and second-order parameters of the points on the contact path of the pinion, which matches with the original wheel flank, can be obtained using the meshing equation. For the corresponding machine-tool settings, the blade angle of the cutter is given as input, and the cutter radius, as well as the quintic polynomial coefficients of each motion axis of the CNC machine, is calculated through solving an equation set. Finally, the pinion member can be cut/ground again with modified machine-tool settings.

## 5 Experiments and results

In this section, the proposed approach was conducted on a ground face-milled hypoid gear pair to demonstrate its effectiveness. The basic geometry parameters are shown in Table 1.

### 5.1 Test 1: design pinion with great maximal TE and short major axis of contact ellipse

In this test, the contact attributes were designed like this: the maximal transmission error was 400  $\mu\text{rad}$ , and the major axis of the instantaneous contact ellipse was 10 mm for the drive side and 7 mm for the coast side. It is evident that the modification both along the contact path and along the contact line is great. The position and direction of the contact path (green line) are shown in Fig. 3a. The contact pattern is designed to be a little close to the toe for the drive side, a little close to the heel and tip for the coast side under light load condition for the reason that as the load increases, the contact pattern will extend to the whole flank.

The rolling test results are shown in Fig. 3d. It can be seen that the real contact pattern is extremely similar to the designed one. Nonetheless, the noise was very loud while this gear pair works, beyond the tolerance limit.

The average flank deviations of the gear pair were obtained via measurement on CMM, the corresponding deviation sum could be calculated. The real ease-off topography was derived by taking flank deviation sum into account. Despite the influence of the deviations, the real ease-off topography deviates little from the designed one, shown in Fig. 3c and b, respectively. In this paper, the values in ease-off topography figures are all expressed in microns on the pinion flank and the contact patterns are all expressed on the wheel flank.

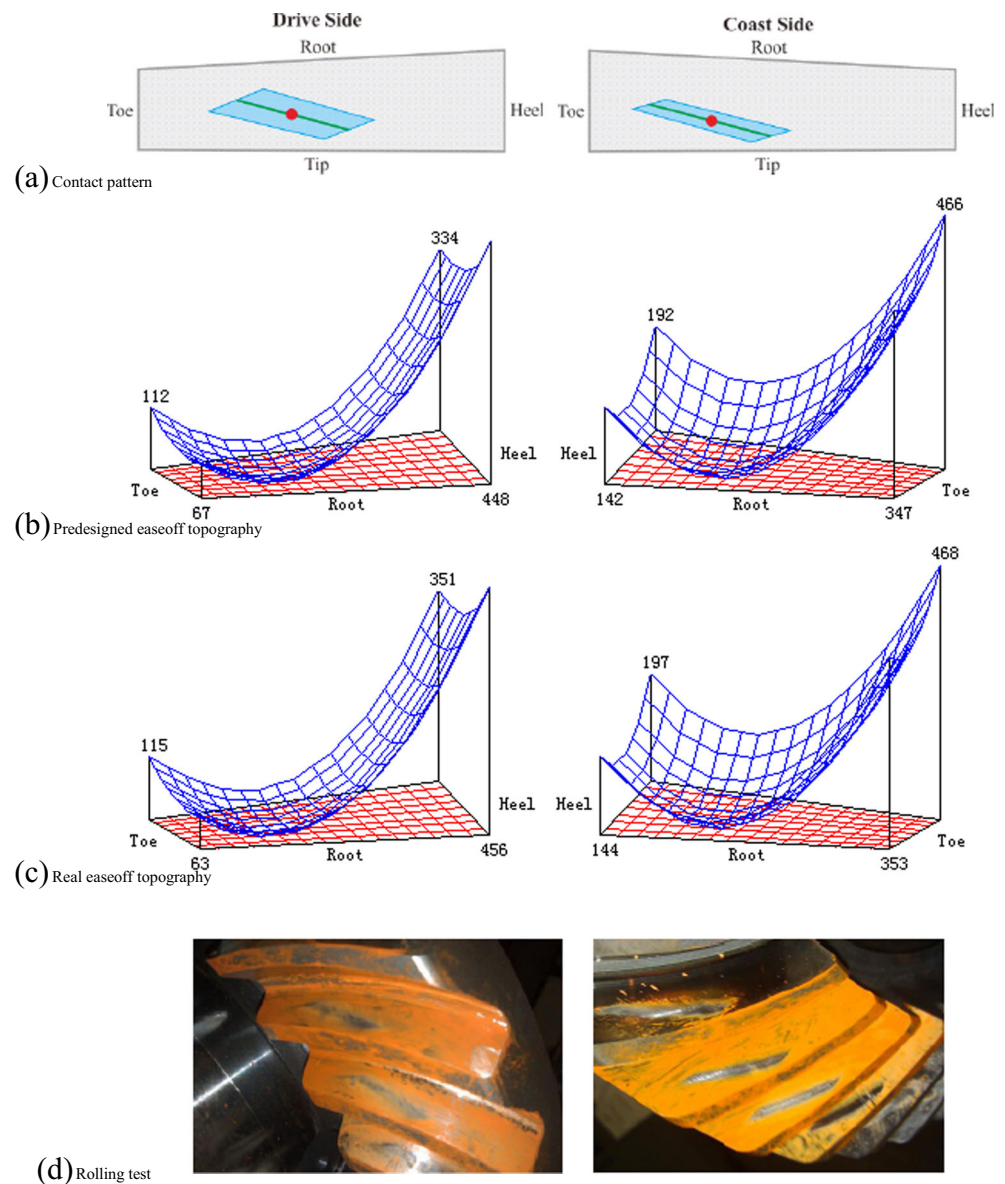
### 5.2 Test 2: design pinion with reduced maximal TE and long major axis of contact ellipse

The maximal transmission error was reduced to 35  $\mu\text{rad}$  this time; at the same time, the major axis of the instantaneous

**Table 1** Basic geometry data of the hypoid gear

	Pinion	Wheel
Offset, mm	26	
Shaft angle, °	90	
Spiral hand	Left	Right
Number of teeth	7	39
Mean spiral angle, °	43.85	35.8333
Average pressure angle, °	22.5	
Pitch angle, °	11.8833	78
Outer cone distance, mm	212.11	217.30
Method	Active design	Formate

**Fig. 3** Design target and experimental results of gear pair with great maximal TE and short major axis of contact ellipse. **a** Contact pattern, **b** predesigned ease-off topography, **c** real ease-off topography, **d** rolling test



contact ellipse was increased to 18 mm for the drive side and 15 mm for the coast side. Obviously, the modification quantity decreases a lot. The position of the contact path was moved 5 mm towards the heel for the coast side.

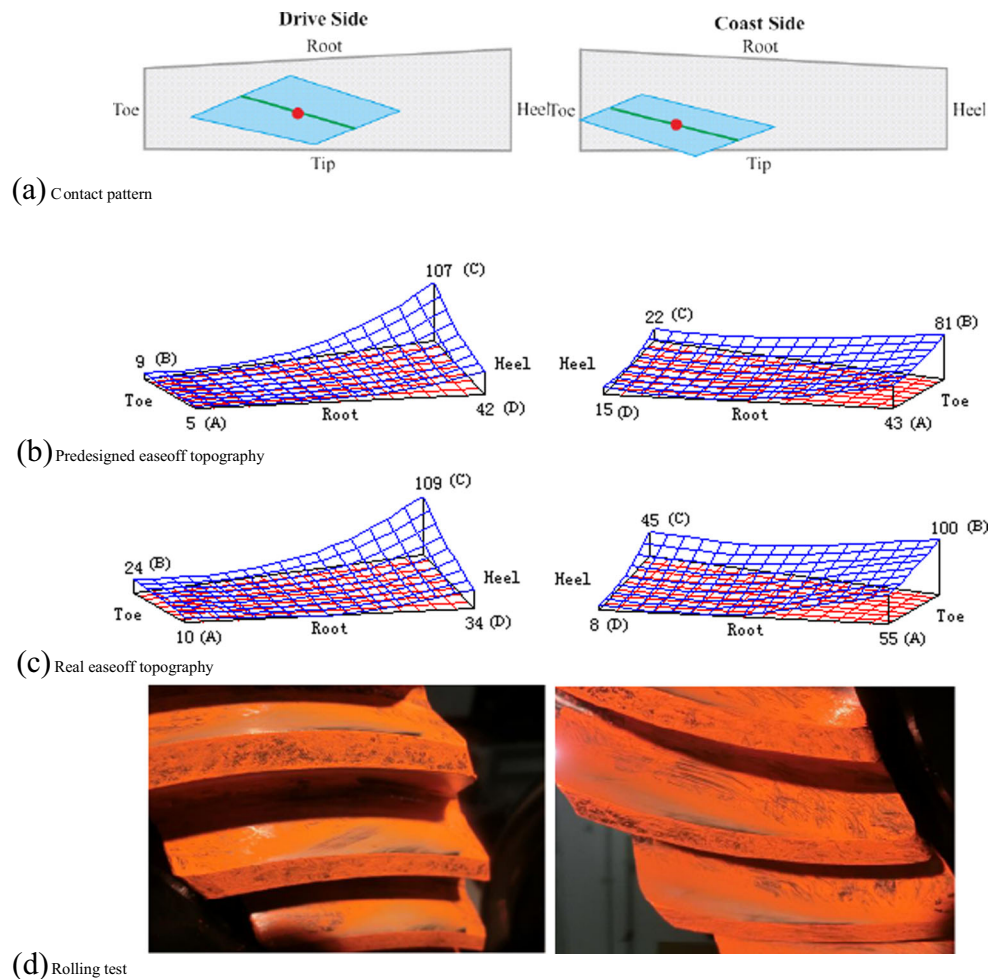
As the rolling test results shown in Fig. 4d, the real contact patterns are far from the designed one, and edge contact occurs, which must be avoided in gear transmission. The situation of the drive side is worse than that of the coast side. And without doubt, the noise was still unfavorable.

The predesigned and the real ease-off topography are shown in Fig. 4b and c, respectively. For the drive side, compared with the predesigned values, the value at the point A on the real ease-off topography increases by  $5 \mu\text{m}$ , and the value at the point B increases by  $15 \mu\text{m}$ , greater than point A. So point A becomes lower relative to point B. The value at point D decreases by  $8 \mu\text{m}$ , and the value at point C increases by

$2 \mu\text{m}$ , so point D becomes lower relative to point C. Hence, the root part becomes lower relative to the tip part on the real ease-off topography. Similarly, point C becomes lower relative to point B and point D becomes lower relative to point A. So, the heel part gets lower relative to the toe part. Accordantly, the lowest part of the real ease-off topography moves towards the heel part and the root part on the pinion flank, and the position of the contact pattern moves towards the heel part and the tip part on the wheel flank.

For the coast side, point D gets lower relative to point C and point A gets lower relative to point B. So the tip part becomes lower relative to the root part. The lowest part moves towards the tip part on the real ease-off topography. Differently, point D gets lower by  $19 \mu\text{m}$  relative to point A, but point C gets higher by  $4 \mu\text{m}$  relative to point B. However, the lowest part moves still towards the heel part on the real ease-off

**Fig. 4** Design target and experimental results of gear pair with reduced maximal TE and long major axis of contact ellipse. **a** Contact pattern, **b** predesigned ease-off topography, **c** real ease-off topography, **d** rolling test



topography because the variation between point D and A is greater than that between point C and B. In addition, the lowest part is closer to the root part, so it gets a larger effect from point D and A on the root line than from point C and B on the tip line. As a result, the position of the contact pattern moves towards the heel part and the tip part on the wheel flank too.

**5.3 Test 3 (a): design pinion with reasonable maximal TE and major axis of contact ellipse**

In this test, the maximal transmission error was still 35  $\mu$ rad, but the major axis of the instantaneous contact ellipse was reduced to 14 mm for the drive side and 10 mm for the coast side. The blade angle for the drive side was changed to obtain a reasonable modification. The position and direction of the contact path remain unchanged.

As the rolling test results shown in Fig. 5d, the contact patterns become improved compared with that in test 2, but still differs from the designed one because of the flank deviations.

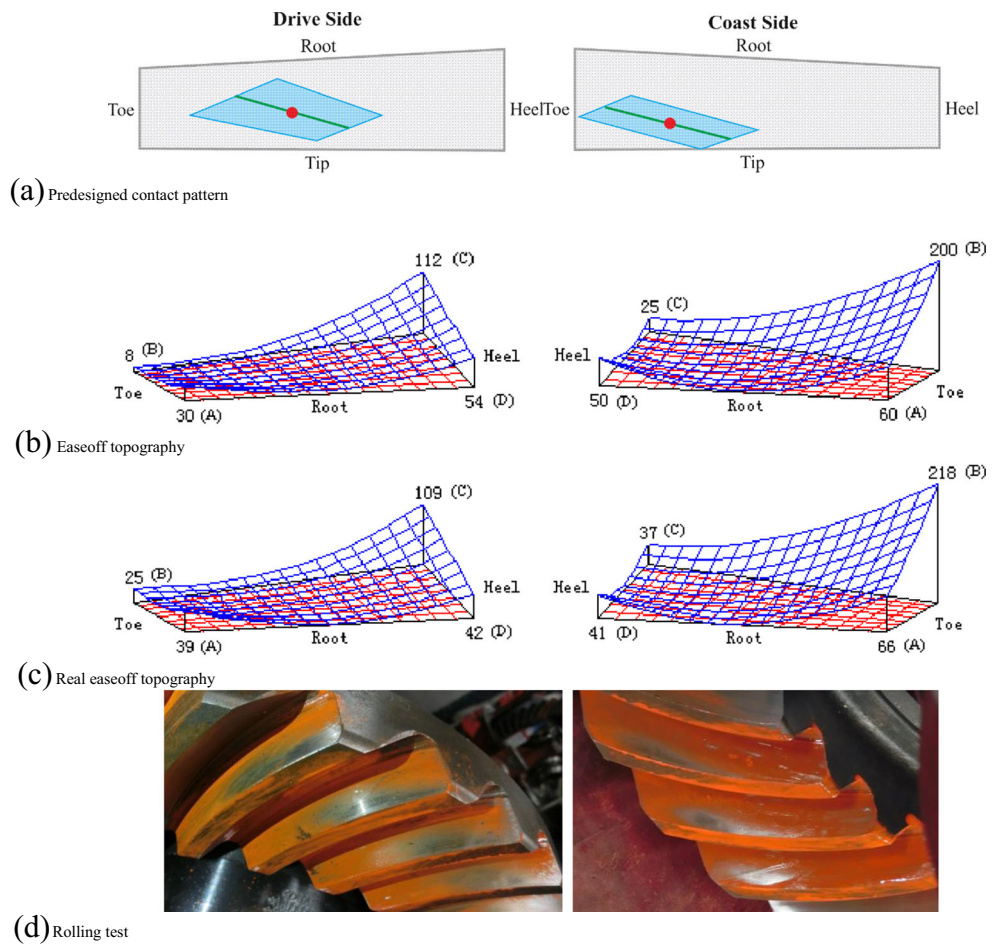
With the same analysis method, compared with the designed ease-off topography, the root part gets lower relative to the tip part on real ease-off topography and the heel part gets lower relative to the toe part, for both the drive side and the coast side. Therefore, the lowest part moves towards the tip and heel part on the wheel flank.

From Fig. 5, it can be derived that the real ease-off topography accords with the rolling test results, with contact pattern deflecting to the heel and the tip on the wheel flank. The noise was a little better than test 1 and test 2, but got worse as load increased.

**5.4 Test 3 (b): redesigning the pinion in test 3 (a)**

To improve the situation in test 3, the flank deviations were considered during the redesign period of the ease-off topography to make sure that the simulated real ease-off topography (shown in Fig. 6a) got close to the original predesigned one, the redesign target (shown in Fig. 5b). For the drive side, the contact path was moved 0.5 mm towards the root of the wheel, the major axis was shortened by 2 mm, and the blade angle for pinion was reduced by 0.005 rad; for the

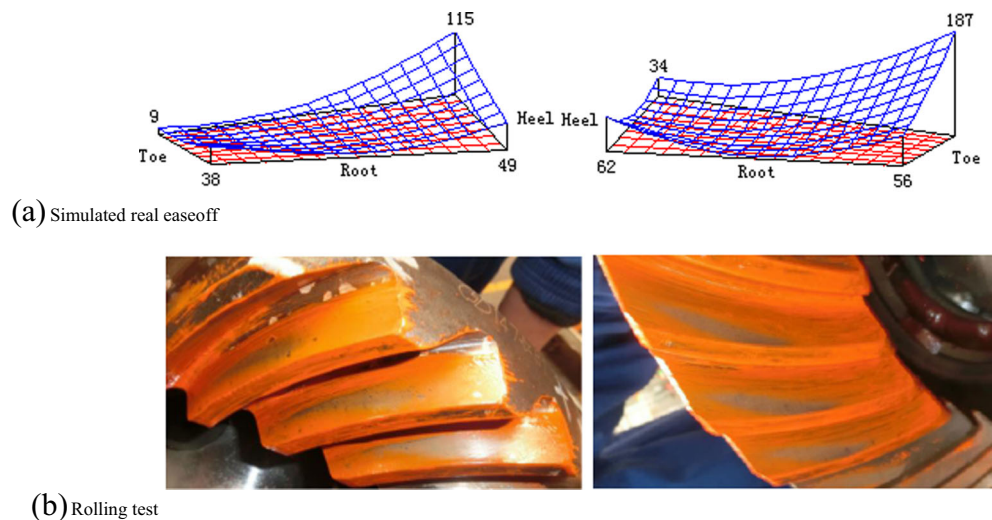
**Fig. 5** Design target and experimental results of gear pair with reasonable maximal TE and major axis of contact ellipse. **a** Contact pattern, **b** predesigned ease-off topography, **c** real ease-off topography, **d** rolling test



coast side, the contact path was moved 1 mm towards the toe of the wheel and 1 mm towards the root of the wheel, and the blade angle for pinion was reduced by 0.005 rad. And then the pinion was ground again using the remodified machine-tool settings on a five-axis machine.

By means of redesign of the pinion, from the rolling test results (shown in Fig. 6b), it can be seen that the real contact pattern get very close to the original designed one (shown in Fig. 5a). The noise was improved much than before, in an acceptable limit.

**Fig. 6** Design target and experimental results after pinion remodification. **a** Simulated real ease-off topography, **b** rolling test





## 6 Discussion

### 6.1 The influence of contact attributes on the flank sensitiveness

Comparing the drive side in test 2 with the drive side in test 3 (a), the major axis of contact ellipse is 18 mm in test 2 and 14 mm in test 3 (a), other conditions are identical. The contact pattern is close to the designed one in test 3 (a) and differs a lot from the designed one in test 2, although the flank deviation magnitude doesn't change much. Similarly, comparing the drive side and the coast side in test 2, the maximal TEs of both sides are the same, and the major axis of contact ellipse for the coast side is shorter by 3 mm than that for the drive side. The rolling test shows that the contact pattern for the coast side is a little closer to the designed one although the situations for both sides are terrible. It can be derived that the longer the major axis of contact ellipse, the more stable the contact pattern.

From the drive side in test 2 to in test 3 (a), the major axis of contact ellipse is shortened by 4 mm and the real contact pattern becomes closer to the designed one. From the drive side in test 3 (a) to test 1, the major axis of contact ellipse is shortened by 4 mm and the maximal TE is increased by  $365 \mu\text{rad}$ , with the result that the real contact pattern becomes extremely similar to the designed one. The improvement is greater than the first comparison, it can be speculated that the increase of the maximal TE is beneficial to the stability of the contact pattern.

However, it is not favorable to increase the modification quantity only, especially along the contact path. For example, in test 1, the maximal transmission error is so great that the impact is heavy at the very moment when the current pair end meshing and the next pair start meshing, which result in the loud noise. The situation in test 2 is that the modification is so little both along the contact path and along the contact line that the edge contact occurs, which leads to loud noise, too. Therefore, reasonable major axis of contact ellipse and maximal TE is needed.

From the analysis in test 2, it can be seen that the contact pattern get more influence from the flank deviations which locate in the vicinity of the contact pattern. For instance, on the coast side in test 2, although point B gets lower relative to point C, the contact area is closer to the tip part on the wheel flank. So the contact pattern is effected more by point D and A than by point B and C, and moves towards the heel part. In most cases, such as pressure angle deviation, spiral angle deviation, crown deviation style, and so on, the flank deviation becomes greater as it gets close to the edge of the flank and usually less in the middle area. Therefore, if the contact pattern is located in the middle area of the flank, it will be more stable. Of course, the position and direction of the contact pattern should be designed according to some other demands simultaneously, like load and misalignment.

### 6.2 The prediction of the contact pattern by the real ease-off topography

In the tests above, no matter the result is excellent or dreadful, the calculated real ease-off topography is similar to the final rolling test result. For instance, in test 1, the real ease-off topography is similar to the designed one, and the real contact pattern accords with the designed one. In test 2, the heel part becomes lower relative to the toe part, and the root part becomes lower relative to the tip part, and the lowest part of the real ease-off topography moves towards the tip and the heel of the pinion flank; similarly, the real contact pattern is in the same condition, far from the designed one. Likewise, in test 3, the contact condition of the real ease-off topography is also similar to the final rolling test tests. Hence, it can be drawn that real ease-off topography can predict the real contact performance of the gear pair, which can be guidance for the design period.

### 6.3 The compensation of the flank deviations through pinion redesign

Although the flank deviations have a negative effect on the contact properties, for example, the real contact pattern will deviates from the designed one, the deviations can be compensated during the pinion redesign period. In test 3 (a), the real contact pattern and the designed one differ because of the flank deviations. In test 3 (b), the flank deviations are compensated when the pinion is redesigned and the real contact pattern is close to the original designed one. Therefore, the detrimental influence of the flank deviations on the contact performance can be reduced a lot by redesigning the real ease-off topography with the flank deviations taken into account, and the recutting/regrinding is conducted on the pinion only, which is advantageous to cost and time saving.

## 7 Conclusion

A pinion development approach is presented to obtain excellent contact performance of the face-milled spiral bevel and hypoid gears by designing and redesigning the pinion flank form by adjusting the contact attributes. Depending on the approach, the pinion is cut/ground based on the original design and the flank deviations are measured. Subsequently, the deviation sum and the real ease-off topography are obtained. According to which, the redesigned ease-off topography is determined. And based on this, the pinion flank is redesigned by readjusting the contact attributes. Finally, the remodified machine-tool settings are calculated by the active design method. In this case, the machine-tool settings are solved directly through an equation set which can guarantee the first-order and second-order parameters of the points on the contact

path of the pinion. Thus, the calculation procedure could increase efficiency and stability to some extent compared with being regarded as a linear regression problem or optimization problem. From the experimental results, some meaningful conclusions can be drawn as follows:

- (1) The contact attributes play an important role on the flank sensitiveness. As the major axis of contact ellipse decreases and the maximal TE increases, the flank sensitiveness decreases. On the contrary, as the major axis of contact ellipse increases and the maximal TE decreases, the flank sensitiveness increases.
- (2) The “real ease-off topography” can predict the real contact pattern and guide design.
- (3) The flank deviations can be compensated through pinion redesign.

The approach could be used for determination of the proper settings and final manufacturing CNC programs for mass production of bevel gears with better meshing properties, if the processing conditions are stable. This paper deals with hypoid gears by half generating method, and this approach could also be applied to other types of face-milled spiral bevel and hypoid gears.

**Acknowledgments** The authors are grateful to the financial support provided by the National Science and Technology Major Project of China under Grant No. 2012ZX04012032 and No. 2013ZX04002-061.

## References

1. Falah AH, Alfares MA, Elkholy AH (2013) Localised tooth contact analysis of single envelope worm gears with assembly errors. *Int J Adv Manuf Technol* 68(9-12):2057–2070
2. Litvin FL, Fuentes A (2004) *Gear geometry and applied theory*, 2nd edn. Cambridge University Press, Cambridge, pp 282–287
3. Suh SH, Jung DH, Lee ES, Lee SW (2003) Modelling, implementation, and manufacturing of spiral bevel gears with crown. *Int J Adv Manuf Technol* 21(10-11):775–786
4. Li XQ, Zhou YF, Wang YZ, Li ZZ (2003) Research on an algorithm for an NC machining hypoid pinion. *Int J Adv Manuf Technol* 22(7-8):491–497
5. Hung CH, Liu JH, Chang SL, Lin HJ (2007) Simulation of gear shaving with considerations of cutter assembly errors and machine setting parameters. *Int J Adv Manuf Technol* 35(3-4):400–407
6. Litvin FL, Kuan C, Wang JC, Handschuh RF, Masseth J, Maruyama N (1992) Minimization of deviations of gear real tooth surfaces determined by coordinate measurements. *J Mech Des* 115(4):995–1001
7. Lin CY, Tsay CB, Fong ZH (1998) Computer-aided manufacturing of spiral bevel and hypoid gears with minimum surface-deviation. *Mech Mach Theory* 33(6):785–803
8. Lin CY, Tsay CB, Fong ZH (2001) Computer-aided manufacturing of spiral bevel and hypoid gears by applying optimization techniques. *J Mater Process Technol* 114(1):22–35(14)
9. Shih YP, Fong ZH (2008) Flank correction for spiral bevel and hypoid gears on a six-axis CNC hypoid generator. *J Mech Des* 130(6):876–877
10. Shih YP, Chen SD (2012) A flank correction methodology for a five-axis CNC gear profile grinding machine. *Mech Mach Theory* 47:31–45
11. Fan Q, DaFoe RS, Swanger JW (2008) Higher-order tooth flank form error correction for face-milled spiral bevel and hypoid gears. *Journal of Mechanical Design* 130(7): 072601-1-7
12. Fan Q (2000) Tooth surface error correction for face-hobbed hypoid gears. *J Mech Des* 132(1):61–69
13. Artoni A, Gabiccini M, Guiggiani M (2008) Nonlinear identification of machine settings for flank form modifications in hypoid gears. *J Mech Des* 130(11):1671–1676
14. Yang Y, Mao SM, Zhao PJ, Guo WC (2014) Correction of tooth surface deviations for aero spiral bevel and hypoid gears. 2014 IEEE/ASME International Conference on Advanced Intelligent Mechatronics
15. Gleason Works Publication (1978) *Understanding Tooth Contact Analysis*. SD3139
16. Shih YP, Fong ZH (2007) Flank modification methodology for face-hobbing hypoid gears based on ease-off topography. *J Mech Des* 129(12):1294–1302
17. Shih YP (2010) A novel ease-off flank modification methodology for spiral bevel and hypoid gears. *Mech Mach Theory* 45(45): 1108–1124
18. Artoni A, Bracci A, Gabiccini M, Guiggiani M (2009) Optimization of the loaded contact pattern in hypoid gears by automatic topography modification. *J Mech Des* 131(1):011008
19. Kolivand M, Kahraman A (2009) A load distribution model for hypoid gears using ease-off topography and shell theory. *Mech Mach Theory* 44(10):1848–1865
20. Kolivand M, Kahraman A (2010) An ease-off based method for loaded tooth contact analysis of hypoid gears having local and global surface deviations. *J Mech Des* 132(7):071004
21. Kolivand M, Li S, Kahraman A (2010) Prediction of mechanical gear mesh efficiency of hypoid gear pairs. *Mech Mach Theory* 45(11):1568–1582
22. Simon VV (2011) Influence of tooth modifications on tooth contact in face-hobbed spiral bevel gears. *Mech Mach Theory* 46(12): 1980–1998
23. Artoni A, Gabiccini M, Guiggiani M, Kahraman A (2011) Multi-objective ease-off optimization of hypoid gears for their efficiency, noise, and durability performances. *J Mech Des* 133(12):121007
24. Artoni A, Gabiccini M, Kolivand M (2013) Ease-off based compensation of tooth surface deviations for spiral bevel and hypoid gears: only the pinion needs corrections. *Mech Mach Theory* 61(1): 84–101
25. Simon V (2013) Design of face-hobbed spiral bevel gears with reduced maximum tooth contact pressure and transmission errors. *Chin J Aeronaut* 26(3):777–790
26. Wu XC (2000) Research on the function-oriented active tooth surface design and advanced manufacturing technology for the curved tooth bevel gears. Dissertation, Xi'an Jiaotong University